Received: 10 May 2022 | Revised: 19 July 2022 | Accepted: 21 July 2022

DOI: 10.1111/jam.15736

Journal of Applied Microbiology sfam

ORIGINAL ARTICLE

Evolution of antibiotic resistance impacts optimal temperature and growth rate in *Escherichia coli* and *Staphylococcus epidermidis*

Portia Mira[1] | **Natalie Lozano-Huntelman**[1] | **Adrienne Johnson**[1] | **Van M. Savage**[1,2,3] | **Pamela Yeh**[1,3]

[1]Department of Ecology and Evolutionary Biology, University of California, Los Angeles, Los Angeles, USA

[2]Department of Computational Medicine, David Geffen School of Medicine, University of California, Los Angeles, Los Angeles, USA

[3]Santa Fe Institute, Santa Fe, New Mexico, USA

Correspondence
Pamela Yeh, Department of Ecology and Evolutionary Biology, University of California, Los Angeles, Los Angeles, USA.
Email: pamelayeh@ucla.edu

Abstract

Aims: Bacterial response to temperature changes can influence their pathogenicity to plants and humans. Changes in temperature can affect cellular and physiological responses in bacteria that can in turn affect the evolution and prevalence of antibiotic-resistance genes. Yet, how antibiotic-resistance genes influence microbial temperature response is poorly understood.

Methods and Results: We examined growth rates and physiological responses to temperature in two species—*E. coli* and *Staph. epidermidis*—after evolved resistance to 13 antibiotics. We found that evolved resistance results in species-, strain- and antibiotic-specific shifts in optimal temperature. When *E. coli* evolves resistance to nucleic acid and cell wall inhibitors, their optimal growth temperature decreases, and when *Staph. epidermidis* and *E. coli* evolve resistance to protein synthesis and their optimal temperature increases. Intriguingly, when *Staph. epidermidis* evolves resistance to Teicoplanin, fitness also increases in drug-free environments, independent of temperature response.

Conclusion: Our results highlight how the complexity of antibiotic resistance is amplified when considering physiological responses to temperature.

Significance: Bacteria continuously respond to changing temperatures—whether through increased body temperature during fever, climate change or other factors. It is crucial to understand the interactions between antibiotic resistance and temperature.

KEYWORDS

antimicrobial resistance, antimicrobials, optimal growth, physiological responses, temperature response

INTRODUCTION

Environmental stressors—such as pH, antibiotics or temperature—affect the growth, replication and physiological welfare of bacterial populations that result in evolutionary trade-offs (Bennett & Lenski, 2007; Deatherage et al., 2017; Duran et al., 2019; Frey et al., 2013; Gething et al., 2010; Lewis et al., 2015; Torda et al., 2017). Each type of stressor plays an important role in the dynamics and prevalence of antibiotic-resistance genes (Al-Nabulsi et al., 2015; Bengtsson-Palme et al., 2018; Letoffe et al., 2014; Li et al., 2020; Mueller et al., 2019; Tan et al., 2019; Yang et al., 2014). For example, cold temperatures, acidic pH and salt stressors increase antibiotic

resistance in *L. monocytogenes* (Al-Nabulsi et al., 2015), and pH impacts the efficacy of antibiotics against resistant pathogens that cause urinary tract infections (Yang et al., 2014) and modifies antibiotic resistance prevalence when elevated (i.e., higher alkalinity) (Letoffe et al., 2014). Antibiotic resistance genes and mobile genetic elements are also less common in saline soils (Tan et al., 2019).

The effects of temperature on the minimum inhibitory concentrations (MICs) of antibiotic-resistant bacteria are highly variable across species. For example, for three bacterial species—*E. coli*, *Salm. enterica* and *Staph. aureus*—the MICs of various antibiotics decrease when exposed to low temperatures but increase when exposed to high temperatures (McMahon et al., 2007). Cold temperatures also result in an increased number of colony-forming units (CFUs) of *Francisella tularensis*, *L. monocytogenes* and *Kl. pneumoniae* resistant to gentamicin at 26°C (compared to 37°C) (Loughman et al., 2016). In agriculture, increased MICs to ampicillin and tetracycline in swine intestinal flora are linked to cold exposure (Moro et al., 1998). For *Ac. baumannii*, an opportunistic pathogen commonly found in hospitals, surface-associated motility was significantly reduced when cooled to 28°C, while biofilm formation on plastic surfaces was increased (De Silva et al., 2018). At 28°C, *Ac. baumanni* was also less susceptible to aztreonam but more susceptible to the combination treatment trimethoprim-sulfamethoxazole (De Silva et al., 2018). Overall, the impact of temperature on MICs is complex and poorly understood because it varies by both species and antibiotic mechanism of action, and the genetic underpinning of these phenotypic responses is unknown (Cruz-Loya et al., 2019; Cruz-Loya et al., 2021; De Silva et al., 2018; Deatherage et al., 2017; Li et al., 2020; Loughman et al., 2016; MacFadden et al., 2018; McGough et al., 2018).

Temperature can also induce physiological responses similar to those caused by some antibiotics (Cruz-Loya et al., 2019). Studies show that high temperatures mimic the effects of aminoglycosides, which inhibit protein synthesis, as well as antibiotics that target DNA or DNA synthesis (Cruz-Loya et al., 2019; Vanbogelen & Neidhardt, 1990). Cruz-Loya et al. (2019) also show that heat-adapted strains become more sensitive to antibiotics that mimic the effects of cooler temperatures, such as DNA gyrase inhibitors (fluoroquinolones) and 30S ribosome inhibitors (tetracyclines), and that heat-shock and cold-shock genes are induced by heat-similar or cold-similar antibiotics. Further studies show that macrolides affect ribosome-mediated protein folding in ways similar to high temperatures (Akerfelt et al., 2010; De Maio, 1999; Kurtz et al., 1986; Mondal et al., 2014; Richter et al., 2010; Stewart & Young, 2004; Vabulas et al., 2010). Overall, these studies suggest that antibiotic mechanisms of action play an important role in bacterial physiological responses at various temperatures.

Given the increasing amount of antibiotics in the environment as a result of human and agricultural use (Butaye et al., 2001; Heuer et al., 2011; Martinez, 2009; Perreten et al., 1997; Zhu et al., 2013) along with changes in body temperature during a fever or global changes in temperature as a result of climate change, it is important to understand how temperature, antibiotics and resistance interact and affect bacterial fitness. Recent studies have investigated the effects of temperature on bacteria after antibiotic resistance has evolved. For example, chloramphenicol-resistant *E. coli* has greater fitness costs at varying temperatures than non-resistant *E. coli* (Herren & Baym, 2022). Another study shows an increase in percentage of antibiotic-resistant pathogens in warmer climates (MacFadden et al., 2018). However, there is almost no study of the reverse question: how is temperature response impacted by the evolution of antibiotic resistance? We investigate how evolved resistance to a range of antibiotics with different mechanisms of action impacts the temperature response, optimal temperature and growth rates in one gram-negative and one gram-positive bacterial species, *E. coli* and *Staph. epidermidis* respectively. Specifically, we ask: (1) Do increasing levels of antibiotic resistance result in shifts in optimal temperature or growth rates? (2) How does cell wall structure influence these shifts? (3) Do antibiotics with similar mechanisms of action induce similar shifts in optimal temperature and growth rates?

MATERIALS AND METHODS

Measuring minimum inhibitory concentrations (MIC) of ancestral strains and evolved isolates

We evolved six independent isolates of *E. coli* (BW25113) (Datsenko & Wanner, 2000) and six independent isolates of *Staph. epidermidis* (ATCC 12228) (Zhang et al., 2003) to 4X the Minimum Inhibitory Concentration (MIC) of each of the antibiotics listed in Table 1. Cultures were grown and evolved in LB media (10 g tryptone, 5 g yeast extract, 10 g NaCl). We first obtained initial IC_{95} values for each species and antibiotic using a 10-step, two-fold serial dilution on 96-well plates – which we refer to as MIC. We inoculated approximately 10^5 cells in each well and allowed them to grow for 22 h at 37°C. We read the endpoint optical density (OD_{600}) using the Tecan Infinite M200 PRO Multimode Microplate Reader and calculated an estimate of the MIC value using the dose–response curve ("*drc*") package in R, version 3.0–1. MIC

Journal of Applied Microbiology

TABLE 1 Antibiotics, abbreviations, ancestral MIC (IC_{95}) and MIC range of evolved isolates evolved with each antibiotic

			Ancestral MIC (μg/ml)		Evolved resistance MIC (μg/ml)	
Gram −/+	Antibiotic	Abbreviation	*E. coli*	*Staph. epidermidis*	*E. coli*	*Staph. epidermidis*
−/+	Amoxicillin	AMX	4.8	0.26	42–237	258–9678
−	Azidothymidine	AZD	0.014	7367.3*	>5000	*
−/+	Ceftazidime	CAZ	0.16	4.9	205–5000	538–10,000
−/+	Cephalexin	CLX	12.4	1.5	680–4110	3753–10,000
−/+	Chloramphenicol	CHL	419.9	85.1	>20,000	827–5000
−	Colistin	COL	0.32	531.8	45–102	840–5000
−/+	Fosfomycin	FOS	0.70	1.09	5–1000	32–1000
+	Gentamicin	GEN	26.4	0.89	423–2264	17–21
−/+	Levofloxacin	LVX	0.064	0.11	0.37–0.535	*
−/+	Meropenem	MER	0.125	0.26	10–90	12–51
−/+	Nitrofurantoin	NIT	14.4	8.4	65–142	483–2000
+	Teicoplanin	TCP	10602.3*	1.02	*	6–221
−/+	Trimethoprim	TMP	0.29	0.54	4–2982	10–5000

Note: The bacterial type (gram-negative or gram-positive) targeted by each drug is listed in the first column followed by the antibiotic name and abbreviation. The MIC for each antibiotic is listed for the ancestral strains of *E. coli* and *Staph. epidermidis*. Evolved resistance MIC columns contain the range of MIC values across the six isolates evolved to each antibiotic. A complete list of evolved MIC values for each biological replicate can be found in Figure S1. Asterisks (*) denote antibiotics that were not used for a particular species because of solubility or evolvability issues during the evolution process.

estimates were determined by the lowest antibiotic concentration observed to inhibit growth by at least 95% (IC_{95}) when compared to the positive control (Table 1, columns 4 and 5).

We also calculated the MICs of all six most resistant isolates (exposed to 4X the ancestral MIC—described in detail below) to their selecting antibiotic to confirm that the identified level of resistance had been achieved (i.e., that the MIC increased to at least 4X the ancestral value). The MIC range for all six evolved isolates can be seen in Table 1, columns 6 and 7 (individual MIC values can be found in Figure S1).

Evolving *E. coli* and *Staph. epidermidis* to 13 antibiotics

We evolved the populations in 96-well plates. Each well was filled with 200 μl of LB media (10 g tryptone, 5 g yeast extract, 10 g NaCl). We began by exposing the strains to 0.125X MIC for 2 days at 37°C. We serial transferred 5 μl of each well to a clean 96-well plate with fresh media and antibiotic daily. Every other day we doubled the concentration of antibiotic (to 0.25X, 0.5X, 1X, 2X and 4X ancestral MIC). We did this for 12 days total, resulting in approximately 120 generations, with 6 independent populations saved at each concentration increase. Each independent population is referred to as an "evolved population." This process resulted in a complete library for each species-antibiotic pair, consisting of 42 unique populations in each library (six evolved populations at each of six concentration steps, plus six replicates of the ancestral populations). We refer to the evolved populations at each concentration step as 'resistance levels'. We created double-library plates that contain all 42 unique populations from *E. coli* and all 42 unique populations from *Staph. epidermidis* (Figure S2). We also evolved ancestral populations in a no-drug environment for 12 days, serial transferring populations daily in fresh LB at 37°C. These populations are referred to as the 'positive control'.

Library purification and confirmation of evolved resistance

Once the populations grew successfully at 4X the ancestral MIC, all evolved populations went through a three-step purification process to confirm their resistance phenotype: First, the 4X populations were inoculated in liquid LB (10 g tryptone, 5 g yeast extract, and 10 g NaCl) with no antibiotic to ensure overnight growth. Second, on the following day, each population was plated on LB agar (LB + 15 g/L agar) containing the antibiotic at the concentration at which they were selected (e.g., 4X MIC populations were plated on LB agar containing 4X the MIC of the ancestral strain). Finally, we considered

the colonies that grew as confirmation of resistance. A single colony from each independent population was picked and again grown overnight in liquid LB only. Each independent isolate was saved in a cryogenic master tube with 25% final concentration of glycerol. Complete double library master plates from the single isolates (*E. coli* + *Staph. epidermidis*) were also saved in a 96-well plate with 25% glycerol (Figure S2). Each double library plate represents both *E. coli* and *Staph. epidermidis* with evolved resistance to the same antibiotic at a range of 0.125X to 4X ancestral MIC, resulting in a total of 14 double library plates—one for each antibiotic used plus one positive control plate evolved for 12 days without antibiotics at 37°C. All experiments were performed on the clonal isolates.

Characterizing temperature response curves and determining optimal temperature

To obtain temperature response curves as resistance evolved, the glycerol double library master plates were thawed at room temperature for 1 h before pinning over to a clean (LB only) 96-well plate. The pinned plate was inoculated at 37°C for 16–18 h to confirm growth, lack of contamination during the pinning process, and that stationary phase was reached so that approximately the same number of cells could be pinned over for the experimental plates. Experimental 96-well plates then were pinned from the fresh double library plates, using three replicate plates per temperature treatment (16°C, 18°C, 22°C, 24°C, 28°C, 30°C, 34°C, 36°C, 38°C, 40°C, 42°C, 44°C, 48°C and 50°C). Because there was a small amount of growth at 50°C in the isolates evolved to amoxicillin, ceftazidime and cephalexin, we also measured optical density at 52°C and 54°C. The endpoint OD_{600} was read between 16–18 h after incubation to characterize the temperature response curves for each biological replicate. All temperature response curves can be found in the supplemental information (Figure S3, Mendeley Data Depository doi: 10.17632/vb25gvtcx4.1).

To describe the resulting temperature responses, we used a model created and described by Cruz-Loya et al. (2021). In brief, this model is a modified Briere model that has been reparametrized as shown in Equation (1). For our purposes, g_{max} is the maximum growth (OD_{600} value), and s and α are parameters that determine the shape of the curve.

$$g(T) = g_{max}\left[\left(\frac{T - T_{min}}{\alpha}\right)^{\alpha}\left(\frac{T_{max} - T}{1-\alpha}\right)^{1-\alpha}\left(\frac{1}{T_{max} - T_{min}}\right)\right]^{s} \quad (1)$$

All three replicates for each experimental plate were pooled together to fit the model using the nls.LM function (part of the minpack.lm package) in R (Bates & Chambers, 1992; Bates & Watts, 1988). Once we fit the data to the model, we used the resulting coefficient values to determine the optimal temperature (T_{opt}), as shown in Equation (2).

$$T_{opt} = \alpha T_{max} + (1 - \alpha)T_{min} \quad (2)$$

Linear regressions and bootstrap analysis

To determine the effects of resistance evolution on optimal temperature, we performed a linear regression on optimal temperature (T_{opt}) and resistance level for each biological replicate using the 'lm' function in R. We used an analysis of variance (ANOVA) to test if species and antibiotic had significant effects on the shifts in optimal temperature. We used the *aov* function in R to compare mean optimal temperatures across resistance levels (isolates evolved to 0.125X, 0.25X, 0.5X, 1X, 2X and 4X ancestral MIC) while considering the variability of species and antibiotics.

We acknowledge that our initial dataset did not meet all the assumptions of the NLS (variance was not homogenous), although we were still able to obtain reasonable fits. To check for the effects of the lack of homogeneity, we plotted the residuals. We observed as the coefficients of the model became larger for *Staph. epidermidis*, i.e., larger values of T_{max} and T_{min} (higher temperatures), the residuals also increased—indicating higher variation. This was most likely a result of heteroscedastic variation in our data. For this reason, we used nonparametric bootstrapping methods (bootstrap with replacement) and applied the NLS for every bootstrap iteration to fit the modified Briere model (Equation 1) and to calculate the optimal temperature (T_{opt}) for each iteration. The optimal temperatures from three experimental replicates were pooled, and then bootstrapping methods were used to determine a 95% confidence interval for each optimal temperature. These confidence intervals describe the range of values that contain 95% of the T_{opt} values from the bootstrap.

Growth rate analysis

For growth rate analysis, double library plates were pinned using the same method as for the temperature response assays. Kinetic calculations were taken by measuring OD_{600} every 30 min for 22 h using the Biotek Epoch2 at 37°C. Growth rates were calculated using the *GrowthRates* program version 4.5 (Hall et al., 2014). *GrowthRates* uses 5

sequential data points of the exponential phase of growth (plotting the natural log of OD_{600} vs. time) and provides correlation coefficients (R) for the calculated linear fits. We only considered growth rates that had correlation coefficients of >0.995 in our analysis. We performed an ANOVA and a Dunnett's test to correct for multiple testing in R to determine any significant differences in growth rates between highest evolved isolates and the ancestral populations. The complete set of growth rate output can be found in Table S1.

RESULTS

We evolved *E. coli* and *Staph. epidermidis* independently to 13 antibiotics and confirmed resistance was achieved through 4- to 20,000-fold increases in MIC values (Table 1). The antibiotics were chosen to span various mechanisms of action because of their availability and solubility. We identified the optimal temperature for each resistance level using a modified Briere model (Cruz-Loya et al., 2021). An example of how the temperature response curves shift as resistance evolves to two different cell wall inhibitors is shown in Figure 1. A list of the optimal temperatures, parameter values and significance can be found in Table S2. To measure confidence intervals, we performed a nonparametric bootstrap analysis (see Methods and Table S3). We confirmed that species and antibiotics have significant impacts on optimal temperature and growth rates by using an analysis of variance (ANOVA), p-values were less than 0.001 for all six evolved isolates (Tables S4 and S5).

Trends in optimal temperature after evolved resistance

We found several patterns in how optimal temperature changes as resistance evolved to the 13 antibiotics in both *E. coli* and *Staph. epidermidis*. Generally, for *E. coli* we found a decrease in optimal temperature as resistance evolved to cell-wall inhibitors and nucleic-acid synthesis inhibitors

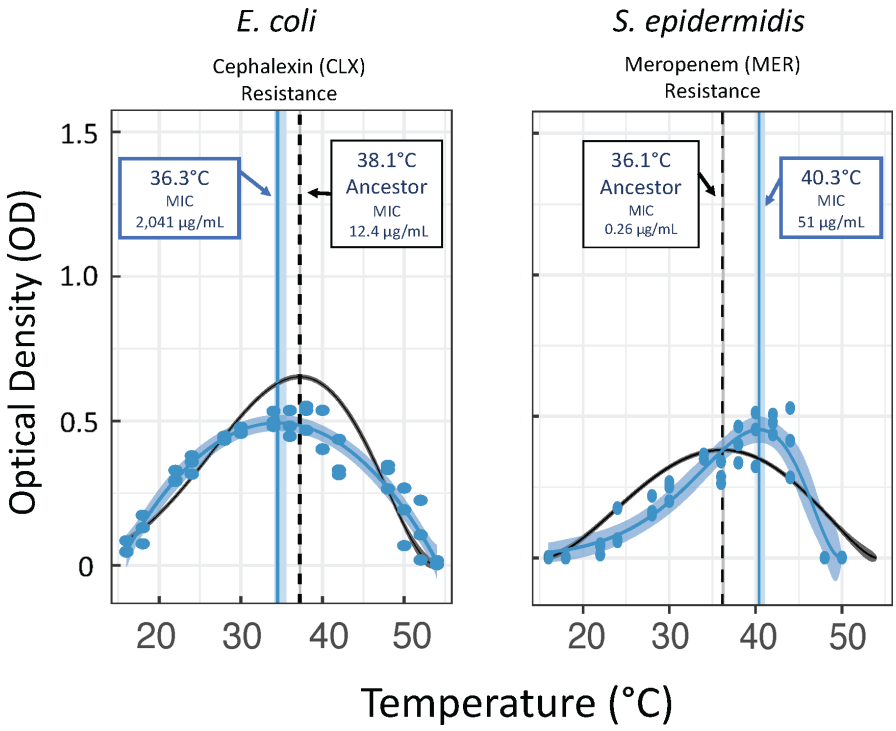

FIGURE 1 Shifts in optimal growth temperature as *Staph. epidermidis* and *E. coli* evolve resistance to cell wall inhibitors. Using a modification of the Briere model (Cruz-Loya et al., 2021), we identified the optimal temperature for each species as resistance evolves. This figure shows the temperature response curve for *E. coli* (left) and *Staph. epidermidis* (right) as they evolve resistance to cephalexin and meropenem, both cell-wall inhibitors. Panels represent the optical density (OD) plotted against temperature (°C) for one biological replicate of each species at the highest resistance levels, MIC shown in boxes. The temperature response curve of the ancestral strain, no resistance (black curve) and the 95% confidence interval via bootstrap (dark grey shaded area) are shown. The CI is hardly visible as the estimate of the curve has low variation. The black dotted vertical line represents the optimal temperature of the ancestral strains—38.1°C for *E. coli* and 36.1°C for *Staph. epidermidis* (full data in Figure S3). The blue data represents single measurements from triplicate experimental runs for one biological replicate. The estimated optimal temperature (blue vertical line), and the 95% confidence interval based on 10,001 bootstrap replicates (blue shaded curve) are shown. The confidence interval goes below the mean value but is challenging to see.

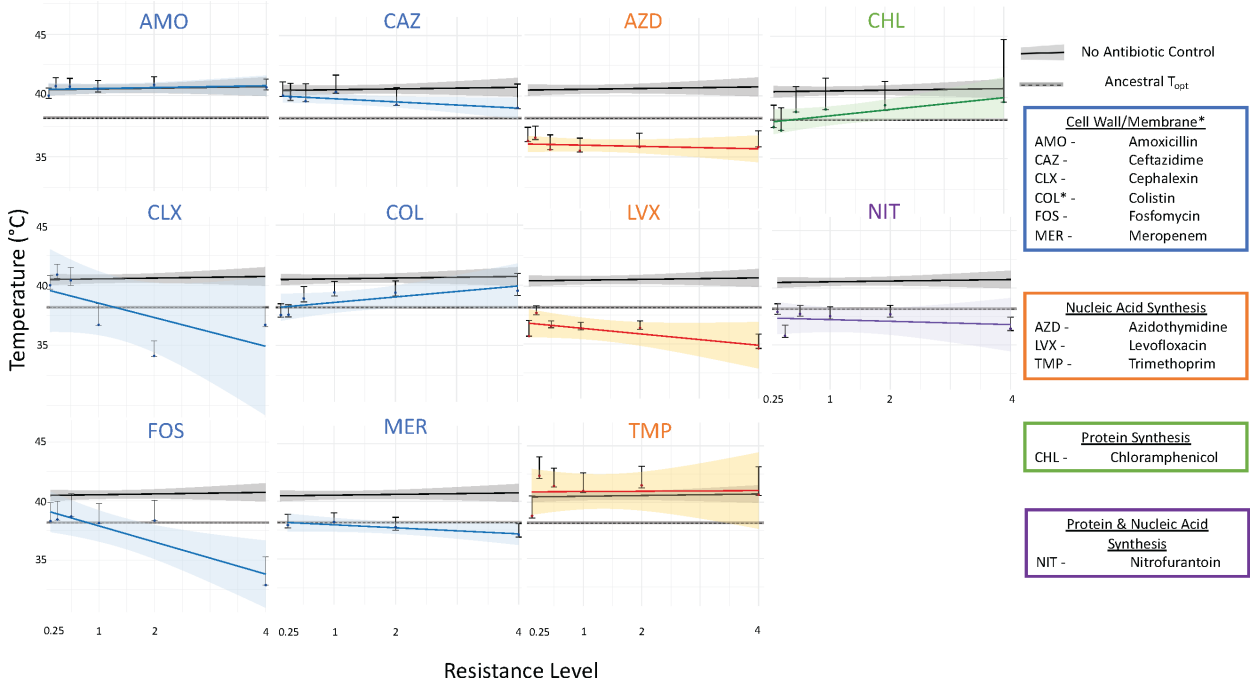

FIGURE 2 Optimal temperature varies depending on antibiotic as resistance evolves in *E. coli*. Optimal temperature in °C (y-axis) plotted against resistance level (x-axis) for *E. coli*. Standard error is shown in the shaded regions and bootstrap confidence intervals are shown by error bars. Panels represent optimal temperature for each resistance level from the lowest level of resistance (isolates exposed to 0.125 times the ancestral MIC) to the highest level of resistance (isolates exposed to four times the ancestral MIC). The first evolved isolates are shown except for GEN (third biological replicate shown). Evolved isolates 2–6 can be found in Figures S4–S9, positive control Figure S16. Antibiotics are colour-coded by mechanism of action. The black line represents the optimal temperatures of the positive controls that were evolved for 12 days without antibiotics. Plots show the optimal temperature of the positive control for days 2, 4, 6, 8, 10 and 12 of being evolved at 37°C without drugs. A linear regression was fit across all data. The shaded area represents the bootstrap confidence interval of the fitted linear regression. The ancestral optimal temperature is shown as a black dotted horizontal line.

(Figure 2-blue and orange trend lines) and an increase in optimal temperature as resistance evolved to protein-synthesis inhibitors (Figure 2-green trend line). On the other hand, when *Staph. epidermidis* evolved resistance, we observed a general increase in optimal temperature across most antibiotics tested, regardless of mechanism of action (Figure 3). It is important to note that both species evolved at a slightly different optimal temperature (37°C) compared to their ancestral optimal temperature, *E. coli* (38.1°C) and *Staph. epidermidis* (36.1°C).

Significant shifts in optimal temperature

To consider the environmental impacts of the evolution process, the optimal temperature was measured on the positive control (ancestral strains evolved at 37°C in no drug environment for 12 days). We noticed a rapid increase in optimal temperature after the first 2 days evolved in no drug environment—from 36.1°C to 40.8°C in *Staph. epidermidis* and from 38.1°C to 40.5°C for *E. coli*. Then, from days 2–12 days, the optimal temperature continued to increase slightly—*E. coli* from 40.5°C to 40.7°C and *Staph. epidermidis* from 40.8°C to 41.7°C (control lines, Figures 2 and 3). Overall, we found the shifts in optimal temperature to be distinctive to the individual antibiotic-evolved isolates. While we observed increasing and decreasing shifts in optimal temperature in both species and many antibiotics, in most evolved isolates, these shifts were not significant (Figure 4, white boxes). When *E. coli* evolved resistance to amoxicillin, ceftazidime, colistin, fosfomycin, meropenem, nitrofurantoin, levofloxacin, azidothymidine and trimethoprim, the optimal temperature significantly decreased in some, but not all, evolved isolates (Figure 4, blue-shaded boxes). Amoxicillin, ceftazidime, colistin, fosfomycin and meropenem are cell wall inhibitors, while nitrofurantoin, levofloxacin, azidothymidine and trimethoprim inhibit nucleic acid synthesis and DNA replication. We also found significant increases in optimal temperature in some *E. coli* isolates when resistance evolved to meropenem, gentamicin, chloramphenicol, nitrofurantoin and azidothymidine (Figure 4, red-shaded boxes). Similar to *E. coli*, when *Staph. epidermidis* evolved resistance, shifts in optimal temperature in most evolved isolates were not significant. However, there were fewer significant shifts compared to *E. coli*. Only

Journal of Applied Microbiology

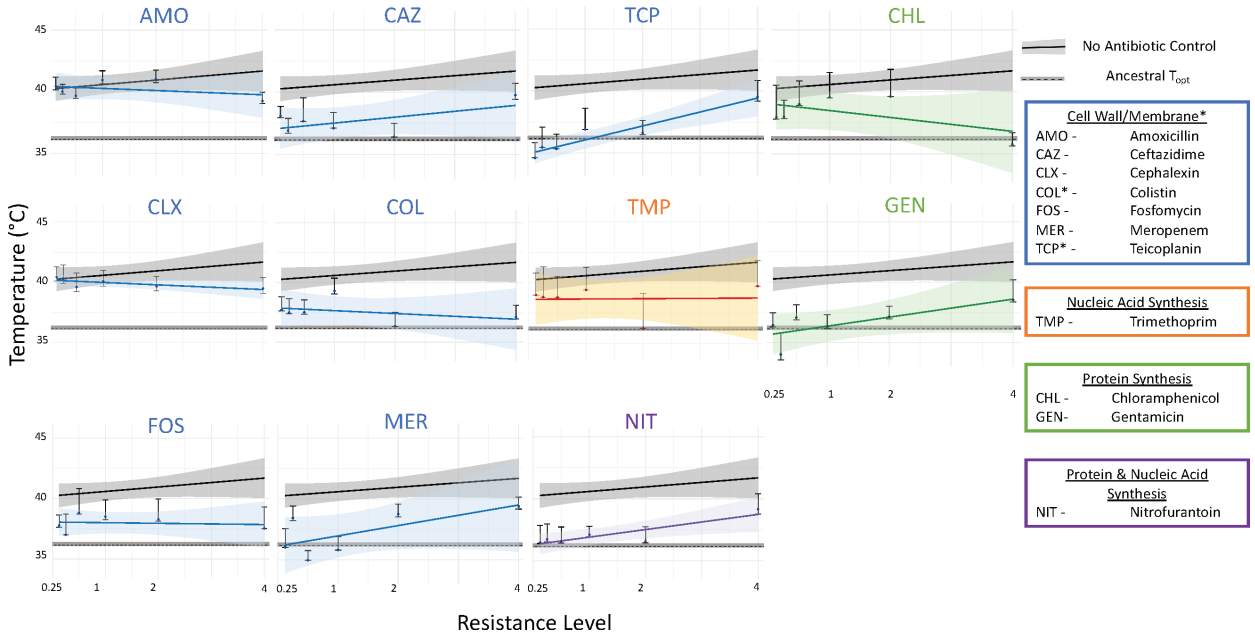

FIGURE 3 Optimal temperature varies depending on antibiotic as resistance evolves in *Staph. epidermidis*. Optimal temperature in °C (y-axis) plotted against resistance level (x-axis) for *Staph. epidermidis*. Standard error is shown in the shaded regions and bootstrap confidence intervals are shown by error bars. Panels represent optimal temperature for each resistance level from the lowest level of resistance (isolates exposed to 0.125 times the ancestral MIC) to the highest level of resistance (isolates exposed to four times the ancestral MIC). The first evolved isolates are shown. Evolved isolates 2–6 can be found in Figures S10–S15, positive control Figure S16. Antibiotics are colour coded by mechanism of action. The black line represents the optimal temperatures of the positive controls that were evolved for 12 days without antibiotics. Plots show the optimal temperature of the positive control for days 2, 4, 6, 8, 10 and 12 of being evolved at 37°C without drugs. A linear regression was fit across all data. The shaded area represents the bootstrap confidence interval of the fitted linear regression. The ancestral optimal temperature is shown as black dotted horizontal line.

three of the 13 antibiotics tested had significant shifts in optimal temperature for *Staph. epidermidis*. Cephalexin had significant decreases, gentamicin had significant increases and colistin had both a significant increase and decrease in optimal temperature (Figure 4, red- and blue-shaded boxes).

Exposure to antibiotics results in an overall lower optimal temperature

When *E. coli* evolved resistance to azidothymidine and levofloxacin, there was a decrease in optimal temperature below ancestral optimal temperature (38.1°C) in all evolved isolates, except isolate 6 for azidothymidine. This also occurred in isolates that evolved to nitrofurantoin, fosfomycin, gentamicin and colistin although some of the confidence intervals overlap with the ancestral optimal temperature (Figure 2; Figures S4–S9a). Although these trends themselves did not significantly decrease as resistance evolved, once isolates were exposed to the lowest concentration of antibiotic, their optimal temperature decreased and remained below the ancestor's optimal temperature. On the other hand, when *Staph. epidermidis* isolates evolved resistance, the optimal temperature remained above the ancestral optimal temperature, 36.1°C (Figure 3; Figures S10–S15). Interestingly, as resistance evolved in *Staph. epidermidis* the optimal temperature also increased, but at a slower rate than the positive control populations, indicating that exposure to the antibiotics slows the change that the environment has on optimal temperature. We also found that the optimal temperature of isolates evolving resistance to amoxicillin and cefalexin overlapped with the positive control (Figures S10–S15).

Influence of species and antibiotic mechanism of action on optimal temperature

We found that shifts in optimal temperature can be species-specific, strain-specific and drug specific. When considering antibiotic mechanism of action, shifts in optimal temperature varied for *E. coli*. For example, nucleic-acid synthesis inhibitors led to both increased (AZD) and decreased (LVX, TMP) optimal temperatures, suggesting that physiological responses to temperature are drug-specific, not mechanism of action specific. The same was true for cell-wall inhibitors for both species (Figure 4). Interestingly, in the case of four antibiotics—meropenem,

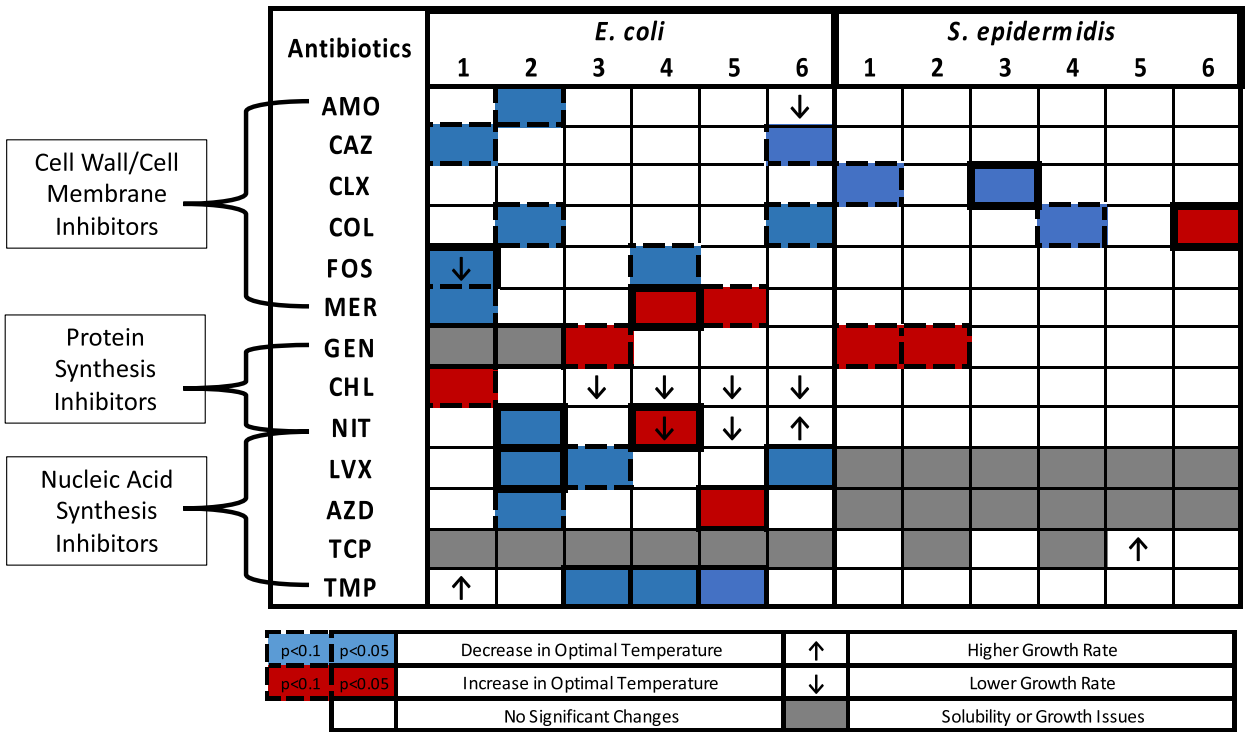

FIGURE 4 Evolved resistance to various classes of antibiotics results in significant changes in growth rate and optimal temperature. Results of six evolved isolates of *E. coli* (left) and *Staph. epidermidis* (right) evolved to 13 antibiotics. Antibiotics are organized by mechanism of action. Nitrofurantoin (NIT) acts both as a protein-synthesis inhibitor and a nucleic-acid synthesis inhibitor. Linear regressions and bootstrap analysis were used to determine shifts in optimal temperature as resistance evolves. Colour-filled boxes represent significant decrease (blue) or a significant increase (red) in optimal temperature as resistance evolves, $p < 0.05$ solid and $p < 0.1$ dashed boxes. ANOVA and a Dunnett's Test were used to compare the growth rates of the ancestral populations to the highest evolved strains (exposed to 4X the ancestral MIC). Significant decreases in growth rates are shown in downward pointing arrows (↓) and significant increases in growth rates are shown in upward pointing arrows (↑) ($p < 0.05$).

nitrofurantoin, azidothymidine (*E. coli*) and colistin (*Staph. epidermidis*)—temperature shifts varied when isolates evolved resistance to the same drug (Figure 4) indicating that responses to temperature are also strain-specific. We also observed species-specific responses. For example, colistin resistance led to a significant decrease in optimal temperature for two evolved isolates of *E. coli* but a significant increase in optimal temperature for one evolved isolate of *Staph. epidermidis* (Figure 4). Finally, we saw some drug-specific responses that were consistent across species. For example, significant increases in optimal temperature when both species evolved resistance to gentamicin, and significant decreases in optimal temperature when both species evolved resistance to colistin (Figure 4).

Changes in growth rate associated with resistance

Using growth rate as a proxy for fitness, we examined if there were significant fitness costs associated with evolved resistance across the 13 antibiotics tested. We compared growth rates of the isolates exposed to 4X the ancestral MIC to the growth rate of the ancestor. We found significant decreases in growth rate as *E. coli* evolved resistance to amoxicillin, fosfomycin, chloramphenicol and nitrofurantoin (Figure 4, downward arrows), and significant increases in the growth rate as *E. coli* evolved resistance to nitrofurantoin and trimethoprim. Only one isolate of *Staph. epidermidis* had a significant increase in growth rate- when resistance evolved to Teicoplanin (Figure 4, upward arrows). Interestingly, we observed no cases in which resistance caused significant decreases in growth rate for *Staph. epidermidis*. Growth rate data can be found in Table S1. To confirm the evolved isolates indeed grew faster, we compared colony forming unit (CFU) counts of two resistant *E. coli* isolates (FOS1 and NIT6) and one resistant *Staph. epidermidis* population (TCP5) to ancestral populations (Figure S17). For the *E. coli* isolates, the CFU counts were higher for NIT6 and lower for FOS1 which supports the quantitative results we observed (Figure 4). However, this was not the case for *Staph. epidermidis*. The teicoplanin-resistant isolate showed a significant increase

in growth rate but had lower overall CFU counts compared to ancestral *Staph. epidermidis* (Figure S17). This result suggests that other factors are impacting the higher OD readings, such as biofilm formation.

DISCUSSION

Our work suggests there exist complex interactions between the evolution of antibiotic resistance, temperature response and growth rates across species. Evolved isolates exhibited shifts in optimal temperature that are drug-specific, species-specific and strain-specific and reflect distinctive differences likely due to pleiotropic effects and epistasis. When *Staph. epidermidis* evolved resistance, we observed significant decreases and increases in optimal temperature or increases in growth rate in seven isolates compared to the ancestor. When *E. coli* evolved resistance, 30 isolates had significant changes - increases or decreases in optimal temperature and/or growth rate, depending on the antibiotic. In both species, shifts in optimal temperature either above or below the ancestral optimal temperature occurred at the lowest level of adapted resistance to most drugs (isolates exposed to 0.125X ancestral MIC); this is likely due to the dual-stressors of antibiotic and temperature and suggests that exposure to even low concentrations of antibiotics can impact physiological responses to temperature.

Typically, the evolution of antibiotic resistance comes with associated fitness costs, such as decreased growth in no-drug environments compared to susceptible counterparts (Andersson, 2006; Andersson & Hughes, 2010; Andersson & Levin, 1999; Gagneux et al., 2006; Melnyk et al., 2015). We found a pattern of different growth-rate responses between gram-negative *E. coli* and gram-positive *Staph. epidermidis*. We suspect these differences are due to the inherent genetic differences that evolved within each independent isolate and are species-specific and strain-specific. Compared to ancestral strains, different *E. coli* isolate's growth rates either increased or decreased significantly as resistance evolved across antibiotics. However, *Staph. epidermidis* only showed one significant increase in growth rate as resistance evolved to Teicoplanin. The latter result is likely due to physiological changes that take place in the cell wall of this gram-positive organism or be due to the isolates adapting to a slightly higher temperature than the ancestral optimal temperature during the evolution process (37°C compared to 36.1°C). As a defence mechanism, *Staph. epidermidis* can replicate without going through binary fission, so the cells containing duplicated chromosomes begin to elongate (Giesbrecht et al., 1998) or can form biofilms that adhere and accumulate on the well of the 96-well plate (Zhou et al., 2015). These mechanisms could result in higher optical density (OD) readings, and therefore faster growth rate measurements, compared to *E. coli* (Al-Kafaween et al., 2019; Fey & Olson, 2010; Zhou et al., 2015). We confirm this may be the case through CFU counts. Even though *Staph. epidermidis* had a significant increase in growth rate when using OD, there was not a significant increase in CFUs compared to the ancestral strain. Not only were there significant differences in growth rates for each species, but we also found significant changes in optimal temperature.

Shifts in optimal temperature differed across antibiotics and evolved isolates as resistance evolved in both *E. coli* and *Staph. epidermidis*. Some antibiotics led to a unidirectional trend, in which all evolved isolates showed the same increasing or decreasing trend. For example, when *E. coli* evolved resistance to chloramphenicol, all evolved isolates increased in optimal temperature. On the other hand, when *E. coli* evolved resistance to cephalexin, all isolates decreased in optimal temperature (Figure 2; Figures S4–S9). Evolved resistance to other antibiotics resulted in a bidirectional trend, where some evolved isolates increased in optimal temperature while others decreased; for example, this occurred when *Staph. epidermidis* evolved resistance to fosfomycin or colistin (Figure 3; Figures S10–S15). These findings suggest apparent genetic diversity in resistance evolution across evolved isolates, resulting in different phenotypic responses to temperature and the large variation in MIC.

Temperatures that are higher than optimal can trigger heat-shock responses from bacterial populations to compensate for possible damage (e.g., protein misfolding) from the increase in temperature (Akerfelt et al., 2010; De Maio, 1999; Neuer et al., 2000; Richter et al., 2010; Vabulas et al., 2010). This response prevents and repairs damages caused by higher temperatures (Vabulas et al., 2010) and, therefore, we expected to find decreases in optimal temperature as resistance evolved. However, we observed that *Staph. epidermidis* had a >1°C increase in optimal temperature in 64% of the isolates adapted to 4X the ancestral MIC as compared to the ancestral strain, like the positive control (no-drug) populations (Tables S2 and S3). All six positive control populations evolved in the no-drug environment, as well as those isolates evolved to fosfomycin, gentamycin, meropenem and nitrofurantoin underwent a 1–5°C increase in optimal temperature. Because this increase also occurred in the no-drug environment, we believe that the accumulation of resistance genes is associated with other physiological responses to the in-vitro environment, such as changes in cell wall structure. Another important factor could be because these isolates were evolved at 37°C, higher than the ancestral optimal temperature of 36.1°C, which could have resulted in mutations occurring within the heat-shock response system

leading to the increase in optimal temperature that we notice after 2 days in the no-drug environment.

We suspect that the evolved *Staph. epidermidis* isolates may have accumulated mutations in genes associated with biofilm formation or cell wall structure, resulting in increases in optical density, more growth at higher temperatures, and faster growth rates. Whether these mutations were a result from antibiotic stress, or temperature stress because they were evolved in a slightly warmer environment compared to ancestral optimal temperature, would require whole-genome sequencing analysis. *Staph. epidermidis* is an important nosocomial pathogen, facilitating infections associated with biomaterials, such as catheters (Fey & Olson, 2010). When exposed to changes in temperature, *Staph. epidermidis* can alter its cell wall structure (Onyango et al., 2012). Temperature changes have also been shown to affect the expression of biofilm formation genes (e.g., icaA, rbf) in another species of *Staphylococcus* (Rode et al., 2007). Similarly, when *P. aeruginosa* and *Ac. baumannii* evolve resistance to tobramycin, mutations occur in two genes associated with biofilm formation, even though neither gene is a direct target of tobramycin (Scribner et al., 2020). We suspect that the initial shift in optimal temperature after the isolates were first exposed to antibiotics could be due to resistant mutations. However, the optimal temperature becomes closer to the positive control optimal temperature as resistance evolves. This could be caused by the accumulation of additional compensatory mutations. *E. coli* also exhibits different phenotypic outcomes as it evolves resistance.

Interestingly, when *E. coli* evolved resistance to nitrofurantoin, there were multiple phenotypic outcomes: we found increases and decreases in optimal temperature as well as increases and decreases in growth rates. In different evolved isolates, resistance to nitrofurantoin resulted in either significant decreases or increases in optimal temperature or significant increases or decreases in growth rate. One possible reason for this variation in response could be due to nitrofurantoin's multiple mechanisms of actions. Nitrofurantoin is a broad-spectrum antibiotic used only to treat carbapenem-resistant infections because it has been shown to induce pulmonary injury (Cassir et al., 2014; De Zeeuw & Gillissen, 2021; Mediavilla et al., 2016). Nitrofurantoin causes nonnative disulfide bonds in the bacterial cell wall (Bandow et al., 2003), damage DNA, and inhibit total protein production in *E. coli* by reacting with ribosomal proteins and rRNA (Thesauraus, 2021). The latter process is followed by the activation of nitrofurantoin by bacterial reductases to highly reactive electrophilic intermediates; an inverse correlation exists between the reductase activity of bacteria and their Nitrofurantoin MIC (Shakti & Veeraraghavan, 2015). Species- and strain-specific mutations and deletions have been identified on nfsA, nfsB and ribE proteins and are associated with high-level nitrofurantoin resistance in Enterobacteriaceae (Sekyere, 2018). The mutations on *nfsA* and *nfsB* genes encode for oxygen-insensitive nitroreductases and hinder the reduction of nitrofurantoin, preventing the formation of the toxic intermediate compounds (Shakti & Veeraraghavan, 2015). Deletions in the *ribE* gene also lead to nitrofurantoin resistance because they inhibit the synthesis of riboflavin, an important cofactor of nfsA and nfsB (Sekyere & Asante, 2018; Vervoort et al., 2014). Because nitrofurantoin has multiple mechanisms of action, resistance can be caused by different mutational pathways leading to resistance, or epistasis. Epistasis has been shown to play a major role in the diversity of antibiotic resistance genes (Levin-Reisman et al., 2019; Mira et al., 2015; Mira et al., 2021; Østman et al., 2012; Santos-Lopez et al., 2019; Schenk et al., 2013). The range of antibiotic mechanism of action and potential epistatic interactions across resistance genes could help explain the multiple phenotypic outcomes observed in nitrofurantoin-resistant *E. coli*.

Our results also support recent work that shows certain antibiotics induce similar physiological responses as hot or cold temperatures (Cruz-Loya et al., 2019). We found that, as resistance evolved to heat-similar or cold-similar antibiotics, isolate's optimal temperature would increase or decrease because of this co-opted adaptation. When isolates evolved resistance to nitrofurantoin, for example, optimal temperature significantly increased from 38.1°C (ancestor) to 38.8°C for one biological replicate of *E. coli*. However, one isolate of *E. coli* that evolved resistance to nitrofurantoin significantly decreased in optimal temperature. Thus, although there is some evidence that antibiotics and temperature induce similar physiological responses, our results suggest that the physiological responses we observed could correspond to specific mutations associated with resistance.

Another result of this work further supports the idea that similar responses can be induced by temperature and antibiotics. When *E. coli* evolved resistance to Levofloxacin (cold-similar drug), optimal temperature significantly decreased across half evolved isolates from 38.1°C (ancestral strain) to between 33.5°C–34.6°C. Levofloxacin falls under the quinolone class of antibiotics and targets DNA gyrase and topoisomerase IV, two enzymes critical in DNA replication, transcription and repair. Mechanisms of quinolone resistance include two types of mutations, with acquisition of resistance-conferring genes occurring in one, or both, of the two main drug target enzymes, resulting in reduced drug binding ability (Aldred et al., 2014; Hooper, 1998; Hooper & Jacoby, 2015; Wang, 1996). Other resistance mutations have been observed in regulatory genes that control the expression of efflux pumps within bacterial

membranes (Aldred et al., 2014; Hooper, 1998). We suspect that one, or both, of the two types of mechanisms of quinolone resistance contribute to decreased optimal temperature in *E. coli*, although DNA sequencing is necessary to confirm this connection.

Climate change and antibiotic resistance are two of the most pressing public health issues the world currently faces. Changes in temperature can drastically influence microorganisms' ability to cause diseases in plants, animals and humans (Baker-Austin et al., 2017; Danovaro et al., 2009; Garcia et al., 2018; Kent et al., 2018; Liang & Gong, 2017). Temperature changes can also influence the evolution of antibiotic resistance, especially given the increased global use of antibiotics (Cruz-Loya et al., 2021; De Silva et al., 2018; Kent et al., 2018; MacFadden et al., 2018; Rodriguez-Verdugo et al., 2020). Our findings show that the presence of antibiotic resistance genes can cause shifts in optimal growth temperature in two bacteria, *E. coli* and *Staph. epidermidis*. We suspect that the genes responsible for resistance can influence heat- or cold-response systems or those epistatic interactions exist between the genes associated with antibiotic resistance and temperature response. Overall, our results show an increase in the complexity of antibiotic resistance when looking at physiological responses to temperature and demonstrate the importance of understanding the interactions between temperature and the evolution of bacterial responses.

ACKNOWLEDGEMENTS

We would like to acknowledge Dr. Sada Boyd for her valuable feedback on the manuscript as well as Dr. Mauricio Cruz-Loya for his support and expertise on the modelling.

CONFLICT OF INTEREST

The authors have no relevant financial or non-financial interests to disclose.

ORCID

Portia Mira https://orcid.org/0000-0003-4093-2809

REFERENCES

Akerfelt, M., Morimoto, R.I. & Sistonen, L. (2010) Heat shock factors: integrators of cell stress, development and lifespan. *Nature Reviews Molecular Cell Biology*, 11, 545–555.

Aldred, K.J., Kerns, R.J. & Osheroff, N. (2014) Mechanism of quinolone action and resistance. *Biochemistry*, 53, 1565–1574.

AL-Kafaween, M.A., Khan, R.S., Hilmi, A.B.M. & Bouacha, M. (2019) Effect of growth media and optical density on biofilm formation by *Staphylococcus epidermidis*. *EC Microbiology*, 15, 277–282.

AL-Nabulsi, A.A., Osaili, T.M., Shaker, R.R., Olaimat, A.N., Jaradat, Z.W., Zain Elabedeen, N.A. et al. (2015) Effects of osmotic pressure, acid, or cold stresses on antibiotic susceptibility of *Listeria monocytogenes*. *Food Microbiology*, 46, 154–160.

Andersson, D.I. & Hughes, D. (2010) Antibiotic resistance and its cost: is it possible to reverse resistance? *Nature Reviews. Microbiology*, 8, 260–271.

Andersson, D.I. & Levin, B.R. (1999) The biological cost of antibiotic resistance. *Current Opinion in Microbiology*, 2, 489–493.

Andersson, D.I. (2006) The biological cost of mutational antibiotic resistance: any practical conclusions? *Current Opinion in Microbiology*, 9, 461–465.

Baker-Austin, C., Trinanes, J., Gonzalez-Escalona, N. & Martinez-Urtaza, J. (2017) Non-cholera vibrios: the microbial barometer of climate change. *Trends in Microbiology*, 25, 76–84.

Bandow, J.E., Brotz, H., Leichert, L.I., Labischinski, H. & Hecker, M. (2003) Proteomic approach to understanding antibiotic action. *Antimicrobial Agents and Chemotherapy*, 47, 948–955.

Bates, D.M. & Chambers, J.M. (1992) *Nonlinear models*. Wadsworth & Brooks/Cole: Statistical Models in S.

Bates, D.M. & Watts, D.G. (1988) *Nonlinear regression analysis and its applications*. Wiley Series in Probability and Statistics, 1st edition. John Wiley and Sons. https://doi.org/10.1002/9780470316757

Bengtsson-Palme, J., Kristiansson, E. & Larsson, D.G.J. (2018) Environmental factors influencing the development and spread of antibiotic resistance. *FEMS Microbiology Reviews*, 42, 68–80.

Bennett, A.F. & Lenski, R.E. (2007) An experimental test of evolutionary trade-offs during temperature adaptation. *Proceedings of the National Academy of Sciences*, 104, 8649–8654.

Butaye, P., Devriese, L.A. & Haesebrouck, F. (2001) Differences in antibiotic resistance patterns of Enterococcus faecalis and Enterococcus faecium strains isolated from farm and pet animals. *Antimicrobial Agents and Chemotherapy*, 45, 1374–1378.

Cassir, N., Rolain, J.M. & Brouqui, P. (2014) A new strategy to fight antimicrobial resistance: the revival of old antibiotics. *Frontiers in Microbiology*, 5, 551.

Cruz-Loya, M., Kang, T.M., Lozano, N.A., Watanabe, R., Tekin, E., Damoiseaux, R. et al. (2019) Stressor interaction networks suggest antibiotic resistance co-opted from stress responses to temperature. *The ISME Journal*, 13, 12–23.

Cruz-Loya, M., Tekin, E., Kang, T.M., Cardona, N., Lozano-Huntelman, N., Rodriguez-Verdugo, A. et al. (2021) Antibiotics shift the temperature response curve of *Escherichia coli* growth. *mSystems*, 6, e00228–e00221.

Danovaro, R., Fonda Umani, S. & Pusceddu, A. (2009) Climate change and the potential spreading of marine mucilage and microbial pathogens in the Mediterranean Sea. *PLoS One*, 4, e7006.

Datsenko, K.A. & Wanner, B.L. (2000) One-step inactivation of chromosomal genes in *Escherichia coli* K-12 using PCR products. *Proceedings of the National Academy of Sciences of the United States of America*, 97, 6640–6645.

De Maio, A. (1999) Heat shock proteins: facts, thoughts, and dreams. *Shock*, 11, 1–12.

De Silva, P.M., Chong, P., Fernando, D.M., Westmacott, G. & Kumar, A. (2018) Effect of incubation temperature on antibiotic resistance and virulence factors of *Acinetobacter baumannii* ATCC 17978. *Antimicrobial Agents and Chemotherapy*, 62, 1514–1517.

De Zeeuw, J. & Gillissen, A. G. 2021. *Nitrofurantoin-induced pulmonary injury* [Online]. UpToDate Available: https://www.uptodate.com/contents/nitrofurantoin-induced-pulmonary-injury [Accessed March 1 2021].

Deatherage, D.E., Kepner, J.L., Bennett, A.F., Lenski, R.E. & Barrick, J.E. (2017) Specificity of genome evolution in experimental populations of *Escherichia coli* evolved at different temperatures. *Proceedings of the National Academy of Sciences of the United States of America*, 114, E1904–E1912.

Duran, R.E., Mendez, V., Rodriguez-Castro, L., Barra-Sanhueza, B., Salva-Serra, F., Moore, E.R.B. et al. (2019) Genomic and physiological traits of the marine bacterium *Alcaligenes aquatilis* QD168 isolated from Quintero Bay, Central Chile, reveal a robust adaptive response to environmental stressors. *Frontiers in Microbiology*, 10, 528.

Fey, P.D. & Olson, M.E. (2010) Current concepts in biofilm formation of *Staphylococcus epidermidis*. *Future Microbiology*, 5, 917–933.

Frey, S.D., Lee, J., Melillo, J.M. & Six, J. (2013) The temperature response of soil microbial efficiency and its feedback to climate. *Nature Climate Change*, 3, 395–398.

Gagneux, S., Long, C.D., Small, P.M., Van, T., Schoolnik, G.K. & Bohannan, B.J. (2006) The competitive cost of antibiotic resistance in Mycobacterium tuberculosis. *Science*, 312, 1944–1946.

Garcia, F.C., Bestion, E., Warfield, R. & Yvon-Durocher, G. (2018) Changes in temperature alter the relationship between biodiversity and ecosystem functioning. *Proceedings of the National Academy of Sciences of the United States of America*, 115, 10989–10994.

Gething, P.W., Smith, D.L., Patil, A.P., Tatem, A.J., Snow, R.W. & Hay, S.I. (2010) Climate change and the global malaria recession. *Nature*, 465, 342–345.

Giesbrecht, P., Kersten, T., Maidhof, H. & Wecke, J. (1998) Staphylococcal cell wall: morphogenesis and fatal variations in the presence of penicillin. *Microbiology and Molecular Biology Reviews*, 62, 1371–1414.

Hall, B.G., Acar, H., Nandipati, A. & Barlow, M. (2014) Growth rates made easy. *Molecular Biology and Evolution*, 31, 232–238.

Herren, C.M. & Baym, M. (2022) Decreased thermal niche breadth as a trade-off of antibiotic resistance. *The ISME Journal*, 16, 1843–1852.

Heuer, H., Schmitt, H. & Smalla, K. (2011) Antibiotic resistance gene spread due to manure application on agricultural fields. *Current Opinion in Microbiology*, 14, 236–243.

Hooper, D.C. & Jacoby, G.A. (2015) Mechanisms of drug resistance: quinolone resistance. *Annals of the New York Academy of Sciences*, 1354, 12–31.

Hooper, D.C. (1998) Bacterial topoisomerases, anti-topoisomerases, and anti-topoisomerase resistance. *Clinical Infectious Diseases*, 27(Suppl 1), S54–S63.

Kent, A.G., Garcia, C.A. & Martiny, A.C. (2018) Increased biofilm formation due to high-temperature adaptation in marine Roseobacter. *Nature Microbiology*, 3, 989–995.

Kurtz, S., Rossi, J., Petko, L. & Lindquist, S. (1986) An ancient developmental induction: heat-shock proteins induced in sporulation and oogenesis. *Science*, 231, 1154–1157.

Letoffe, S., Audrain, B., Bernier, S.P., Delepierre, M. & Ghigo, J.M. (2014) Aerial exposure to the bacterial volatile compound trimethylamine modifies antibiotic resistance of physically separated bacteria by raising culture medium pH. *mBio*, 5, e00944–e00913.

Levin-Reisman, I., Brauner, A., Ronin, I. & Balaban, N.Q. (2019) Epistasis between antibiotic tolerance, persistence, and resistance mutations. *Proceedings of the National Academy of Sciences of the United States of America*, 116, 14734–14739.

Lewis, J.D., Chen, E.Z., Baldassano, R.N., Otley, A.R., Griffiths, A.M., Lee, D. et al. (2015) Inflammation, antibiotics, and diet as environmental stressors of the gut microbiome in pediatric crohn's disease. *Cell Host & Microbe*, 18, 489–500.

Li, M.M., Ray, P., Teets, C., Pruden, A., Xia, K. & Knowlton, K.F. (2020) Short communication: Increasing temperature and pH can facilitate reductions of cephapirin and antibiotic resistance genes in dairy manure slurries. *Journal of Dairy Science*, 103, 2877–2882.

Liang, L. & Gong, P. (2017) Climate change and human infectious diseases: a synthesis of research findings from global and spatio-temporal perspectives. *Environment International*, 103, 99–108.

Loughman, K., Hall, J., Knowlton, S., Sindeldecker, D., Gilson, T., Schmitt, D.M. et al. (2016) Temperature-dependent gentamicin resistance of *Francisella tularensis* is mediated by uptake modulation. *Frontiers in Microbiology*, 7, 37.

Macfadden, D.R., Mcgough, S.F., Fisman, D., Santillana, M. & Brownstein, J.S. (2018) Antibiotic resistance increases with local temperature. *Nature Climate Change*, 8, 510–514.

Martinez, J.L. (2009) Environmental pollution by antibiotics and by antibiotic resistance determinants. *Environmental Pollution*, 157, 2893–2902.

Mcgough, S.F., Macfadden, D.R., Hattab, M.W., Molbak, K. & Santillana, M. (2018) Rates of increase of antibiotic resistance and ambient temperature in Europe: a cross-national analysis of 28 countries between 2000-2016. *Euro Surveillance*, 45(25), 1–12.

Mcmahon, M.A., Xu, J., Moore, J.E., Blair, I.S. & Mcdowell, D.A. (2007) Environmental stress and antibiotic resistance in food-related pathogens. *Applied and Environmental Microbiology*, 73, 211–217.

Mediavilla, J.R., Patrawalla, A., Chen, L., Chavda, K.D., Mathema, B., Vinnard, C. et al. (2016) Colistin- and carbapenem-resistant *Escherichia coli* harboring mcr-1 and blaNDM-5, causing a complicated urinary tract infection in a patient from the United States. *mBio*, 7(4), e01191–16.

Melnyk, A.H., Wong, A. & Kassen, R. (2015) The fitness costs of antibiotic resistance mutations. *Evolutionary Applications*, 8, 273–283.

Mira, P.M., Østman, B., Guzman-Cole, C., Sindi, S. & Barlow, M. (2021) Adaptive processes change as multiple functions evolve. *Antimicrobial Agents and Chemotherapy*, 65, e01990-20.

Mira, P.M., Meza, J.C., Nandipati, A. & Barlow, M. (2015) Adaptive landscapes of resistance genes change as antibiotic concentrations change. *Molecular Biology and Evolution*, 32, 2707–2715.

Mondal, S., Pathak, B.K., Ray, S. & Barat, C. (2014) Impact of P-Site tRNA and antibiotics on ribosome mediated protein folding: studies using the *Escherichia coli* ribosome. *PLoS One*, 9, e101293.

Moro, M.H., Beran, G.W., Hoffman, L.J. & Griffith, R.W. (1998) Effects of cold stress on the antimicrobial drug resistance of *Escherichia coli* of the intestinal flora of swine. *Letters in Applied Microbiology*, 27, 251–254.

Mueller, E.A., Egan, A.J., Breukink, E., Vollmer, W. & Levin, P.A. (2019) Plasticity of *Escherichia coli* cell wall metabolism promotes fitness and antibiotic resistance across environmental conditions. *eLife*, 8, e40754.

Neuer, A., Spandorfer, S.D., Giraldo, P., Dieterle, S., Rosenwaks, Z. & Witkin, S.S. (2000) The role of heat shock proteins in reproduction. *Human Reproduction Update*, 6, 149–159.

Onyango, L.A., Dunstan, R.H., Gottfries, J., von Eiff, C. & Roberts, T.K. (2012) Effect of low temperature on growth and ultrastructure of *Staphylococcus* spp. *PLoS One*, 7, e29031.

Perreten, V., Schwarz, F., Cresta, L., Boeglin, M., Dasen, G. & Teuber, M. (1997) Antibiotic resistance spread in food. *Nature*, 389, 801–802.

Richter, K., Haslbeck, M. & Buchner, J. (2010) The heat shock response: life on the verge of death. *Molecular Cell*, 40, 253–266.

Rode, T.M., Langsrud, S., Holck, A. & Moretro, T. (2007) Different patterns of biofilm formation in *Staphylococcus aureus* under food-related stress conditions. *International Journal of Food Microbiology*, 116, 372–383.

Rodriguez-Verdugo, A., Lozano-Huntelman, N., Cruz-Loya, M., Savage, V. & Yeh, P. (2020) Compounding effects of climate warming and antibiotic resistance. *iScience*, 23, 101024.

Santos-Lopez, A., Marshall, C.W., Scribner, M.R., Snyder, D.J. & Cooper, V.S. (2019) Evolutionary pathways to antibiotic resistance are dependent upon environmental structure and bacterial lifestyle. *eLife*, 8, e47612.

Schenk, M.F., Szendro, I.G., Salverda, M.L., Krug, J. & De Visser, J.A. (2013) Patterns of Epistasis between beneficial mutations in an antibiotic resistance gene. *Molecular Biology and Evolution*, 30, 1779–1787.

Scribner, M.R., Santos-Lopez, A., Marshall, C.W., Deitrick, C. & Cooper, V.S. (2020) Parallel evolution of tobramycin resistance across species and environments. *mBio*, 11(3), e00932–20.

Sekyere, J.O. & Asante, J. (2018) Emerging mechanisms of antimicrobial resistance in bacteria and fungi: advances in the era of genomics. *Future Microbiology*, 13, 241–262.

Sekyere, J.O. (2018) Genomic insights into nitrofurantoin resistance mechanisms and epidemiology in clinical Enterobacteriaceae. *Future Science OA*, 4, FSO293.

Shakti, L. & Veeraraghavan, B. (2015) Advantage and limitations of nitrofurantoin in multi-drug resistant Indian scenario. *Indian Journal of Medical Microbiology*, 33, 477–481.

Stewart, G.R. & Young, D.B. (2004) Heat-shock proteins and the host-pathogen interaction during bacterial infection. *Current Opinion in Immunology*, 16, 506–510.

Tan, L., Wang, F., Liang, M., Wang, X., Das, R., Mao, D. et al. (2019) Antibiotic resistance genes attenuated with salt accumulation in saline soil. *Journal of Hazardous Materials*, 374, 35–42.

Thesauraus, N. 2021. *Nitrofurantoin* [Online]. National Cancer Institute Available: https://ncit.nci.nih.gov/ncitbrowser/ConceptReport.jsp?dictionary=NCI_Thesaurus&ns=NCI_Thesaurus&code=C29293 [Accessed February 23 2021].

Torda, G., Donelson, J.M., Aranda, M., Barshis, D.J., Bay, L., Berumen, M.L. et al. (2017) Rapid adaptive responses to climate change in corals. *Nature Climate Change*, 7, 627–636.

Vabulas, R.M., Raychaudhuri, S., Hayer-Hartl, M. & Hartl, F.U. (2010) Protein folding in the cytoplasm and the heat shock response. *Cold Spring Harbor Perspectives in Biology*, 2, a004390.

Vanbogelen, R.A. & Neidhardt, F.C. (1990) Ribosomes as sensors of heat and cold shock in *Escherichia coli*. *Proceedings of the National Academy of Sciences of the United States of America*, 87, 5589–5593.

Vervoort, J., Xavier, B.B., Stewardson, A., Coenen, S., Godycki-Cwirko, M., Adriaenssens, N. et al. (2014) An in vitro deletion in ribE encoding lumazine synthase contributes to nitrofurantoin resistance in *Escherichia coli*. *Antimicrobial Agents and Chemotherapy*, 58, 7225–7233.

Wang, J.C. (1996) DNA topoisomerases. *Annual Review of Biochemistry*, 65, 635–692.

Yang, L., Wang, K., Li, H., Denstedt, J.D. & Cadieux, P.A. (2014) The influence of urinary pH on antibiotic efficacy against bacterial uropathogens. *Urology*, 84(731), e1–e7.

Zhang, Y.Q., Ren, S.X., Li, H.L., Wang, Y.X., Fu, G., Yang, J. et al. (2003) Genome-based analysis of virulence genes in a non-biofilm-forming *Staphylococcus epidermidis* strain (ATCC 12228). *Molecular Microbiology*, 49, 1577–1593.

Zhou, G., Shi, Q.S., Huang, X.M. & Xie, X.B. (2015) The three bacterial lines of defense against antimicrobial agents. *International Journal of Molecular Sciences*, 16, 21711–21733.

Zhu, Y.G., Johnson, T.A., Su, J.Q., Qiao, M., Guo, G.X., Stedtfeld, R.D. et al. (2013) Diverse and abundant antibiotic resistance genes in Chinese swine farms. *Proceedings of the National Academy of Sciences of the United States of America*, 110, 3435–3440.

Østman, B., Hintze, A. & Adami, C. (2012) Impact of epistasis and pleiotropy on evolutionary adaptation. *Proceedings of the Biological Sciences*, 279, 247–256.

SUPPORTING INFORMATION

Additional supporting information can be found online in the Supporting Information section at the end of this article.

How to cite this article: Mira, P., Lozano-Huntelman, N., Johnson, A., Savage, V.M. & Yeh, P. (2022) Evolution of antibiotic resistance impacts optimal temperature and growth rate in *Escherichia coli* and *Staphylococcus epidermidis*. *Journal of Applied Microbiology*, 133, 2655–2667. Available from: https://doi.org/10.1111/jam.15736